



# Hematoporphyrin Is a Promising Sensitizer for Dual-Frequency Sono-photodynamic Therapy in Mice Breast Cancer

Tahereh Khani<sup>1</sup>, Majid Jadidi<sup>1\*</sup>, Hadi Hasanzadeh<sup>1</sup>, Shima Moshfegh<sup>1</sup>, Shima Saeedi<sup>1</sup>, Shoka Shahryari<sup>1</sup> and Raheb Ghorbani<sup>2</sup>

<sup>1</sup>Department of Medical Physics, Semnan University of Medical Sciences, Semnan, Iran

<sup>2</sup>Social Determinants of Health Research Center, Semnan University of Medical Sciences, Semnan, Iran

\*Corresponding author: Department of Medical Physics, Semnan University of Medical Sciences, Semnan, Iran. Email: jadidim@semums.ac.ir

Received 2021 February 13; Revised 2022 February 05; Accepted 2022 February 12.

## Abstract

**Background:** The combination of sonodynamic and photodynamic therapy (SPDT) may be a new hopeful non-invasive method for cancer treatment, which incorporates a combination of low-intensity ultrasound, laser radiation, and a sensitizer agent.

**Objectives:** This study aimed at evaluating the effects of hematoporphyrin (HP)-mediated SPDT (dual-frequency ultrasound and laser radiation) in the management of mice breast adenocarcinoma.

**Methods:** One hundred and thirty-two female mice with implanted tumors were divided into 22 groups, including sham, laser, 4 groups of dual-frequency ultrasound/laser radiation, 8 groups of HP-mediated SPDT (2.5 and 5 mg/kg), and 8 groups of HP encapsulated in mesoporous silica nanoparticles (HP-MSNs)-mediated SPDT. The sensitizer was administered by intraperitoneal injection and after a 24-hour delay, tumor grafted mice were treated with a combination of dual-frequency ultrasound and laser light. The tumor growth factors were used to assess the treatment outcome.

**Results:** The results indicated that HP or HP-MSNs-mediated SPDT had a delaying tumor growth effect. In the groups treated with dual-frequency ultrasound and laser radiation, the maximum tumor growth inhibition (TGI) ratio was 47.5%, while the maximum TGI ratio in the SPDT groups was 61.6%. The time of T2 and T5 in the case of HP-MSNs-mediated SPDT groups was increased compared with sham and that of HP-mediated SPDT groups ( $P < 0.05$ ). The inhibition ratio on tumor growth increased in all SPDT groups at 12 days after the treatment. Analysis of experimental data demonstrates that this increase was not declined and persisted over 30 days of treatment. The results indicated that SPDT is effective in relative tumor volume when compared with the sham group ( $339.1 \pm 161$  and  $1510.8 \pm 160$ , respectively). HP or HP-MSNs-mediated SPDT groups had Grade I (low), while others had Grade III (high) malignancy in the histological study of mice breast adenocarcinoma.

**Conclusions:** The results revealed that when sensitized by dual-frequency SPDT, hematoporphyrin (with and without MSNs), has a promising effect at delaying tumor growth on mice breast cancer. Therefore, it can be appreciated that careful selection of the sensitizer with SPDT will play an eminent role in the success of cancer therapies.

**Keywords:** Hematoporphyrin, Sonodynamic Therapy, Photodynamic Therapy

## 1. Background

Among the conventional therapeutic procedures of cancer, sonodynamic and photodynamic therapy (SPDT), which incorporates a combination of ultrasound, laser, and a sensitizer agent offered a route toward a non-invasive method. Photodynamic therapy (PDT) is an inventive minimally invasive therapy that is applied as a substitute protocol for the management of cancer. It is based on the buildup of a nontoxic photosensitizer (PS) that is excited by light and reacts with oxygen to generate singlet oxygen, radicals, and triplet species in tumor tissue, the consequence of which is the initiation of cell death

mechanisms (1, 2). The photosensitizer is one of the basic components of PDT, despite light and oxygen (2). Accidentally discovered PDT by Dougherty has proved the value of porphyrin compounds in oncologic suitable photosensitizers (3). The first generation of PDT sensitizers that was approved by the Food and Drug Administration (FDA) (Photofrin) produced singlet oxygen for cancer treatment (4). PDT has not caused DNA damage, mutations, and carcinogenesis, since most PSs do not accumulate in cell nuclei. Although PDT is very safe in the tissues around the cancer region, the light penetration depth is limited and often produces less success (5). Therefore, the wavelength range between 600 and 800 nm with depth penetration of about

8 mm into the tissues has been determined as the practical “therapeutic window” for clinical PDT. Lasers as a standard light source for PDT are monochrome and have high luminance (6). The findings of Banerjee et al.’s study confirmed a potential role for PDT with verteporfin and laser (690 nm) in the management of early breast cancer in 12 female patients (1). Secret et al. proposed that PDT with porphyrin delivery by porous silicon nanoparticles can improve the treatment of breast cancer cells (7, 8).

Since 1989, a novel promising non-invasive approach based on PDT was established with similar principles to PDT. Sonodynamic therapy (SDT) involves the use of ultrasound radiation and a sonosensitizer agent that can be activated by ultrasound. Therefore, SDT overcomes the major limitation of PDT (9). On the other hand, SDT as a non-invasive method for cancer treatment has a deeper penetration ability into the cancer tissue and effectively increases cytotoxicity (10). In SDT, ultrasound exposure utilizes an appropriate frequency and intensity (1 - 3 MHz, 0.5 - 3 W/cm<sup>2</sup>). These waves interact with sonosensitizing agents and as a result, produce free radicals, which cause apoptosis of cancer cells. This activation is related to the cavitation process (11-13), which involves the formation, growth, and exploding of gas-filled bubbles in fluids (9, 14).

As an SDT sensitizer, hematoporphyrin (HP) can maximize the ultrasound effects. On the other hand, porphyrin-based molecules are easily condensed into physiological environments due to their low water solubility (15). Nanoparticles, as a drug delivery system, can easily penetrate cell dams (such as membranes) and effectively accumulate the drug within the tumor tissue. Mesoporous silica nanoparticles (MSNs) have been considered within the field of treatment and diagnosis. For the discharge of the drug-loaded into the mesoporous nano-carriers, the external stimulus of ultrasound is extremely much considered because, in addition to activating sensitivities, it allows the spatial and temporal control of drug release at the specified location, hence increasing therapeutic benefits (16-18). Nevertheless, in a hypoxic tumor medium, the competency of SDT and PDT is low that limits their applications (19). To overcome the aforementioned limitations of these two treatment modalities, the combination of SPDT can help to get a reasonable anti-tumor effect because of the ultrasound good tissue penetration, and focusing of its energy into the specific depth of biological tissue (4).

The sono-photodynamic therapy (SPDT) depended on the accumulation of sensitizer in tumor sight and cytotoxicity enhancement after activation by light or ultrasound. Besides the singlet oxygen production in PDT, mechanical stress, cavitation, and multiple reactive oxygen species are generated in SDT (4). It is concluded that dual-frequency

ultrasound produces more active bubbles and enhances cytotoxic effects when compared with a single-frequency ultrasound. Dual-frequency ultrasound causes the drug to discharge from the carriers and increases drug release into the aqueous environment, which increases cancer cell death (20-22).

## 2. Objectives

SPDT performance, as a minimally invasive cancer treatment, was dependent on the accumulation of sensitizer in tumor sight and cytotoxicity enhancement after activation by ultrasound and laser radiation. The aim of the current research was to evaluate the effects of Hematoporphyrin-mediated SPDT in the management of breast adenocarcinoma. Therefore, the therapeutic effect of sensitized HP and HP-MSNs with the combination of dual-frequency ultrasound (1 and 3 MHz) and laser light (650 nm) in the treatment of Inbred Balb/C mice grafted breast adenocarcinoma were assessed. Tumor volume was measured during 30 days, and the parameters related to tumor growth, animal survival, and histopathological study were recorded.

## 3. Methods

### 3.1. Chemicals

HP 50% (Sigma-Aldrich, Canada) was dissolved in phosphate-buffered saline (PBS, pH = 7.4) and stored in the dark at 4°C. The synthesis of MSNs was performed in the sol-gel process by application of an alkoxide precursor (tetraethyl orthosilicate (TEOS)), and a surfactant (cetyltrimethylammonium bromide (CTAB)). This method consists of the formation of mesoporous nanoparticles under the size range of 60 nm to 1000 nm. The particles were dried at room temperature and calcined at 550°C for 3 h. Subsequently, HP solution was placed adjacent to synthesized nanoparticles. The HP enters into the MSN cavities passively process (23, 24).

### 3.2. Tumor Model

To use a syngeneic tumor model, the confirmed murine spontaneous breast adenocarcinoma was got rid of from anesthetized Balb/C mice (ketamine/xylazine, 30 mg/kg, IP). The tumor tissue was chopped into fresh pieces with a diameter of 2 mm to 3 mm in PBS. A portion of the tumor was subcutaneously placed in the inguinal area of the receptor animal (Inbred Balb/C female mice, 6-8 week-old), and suture clips were used to close the incision. To prevent mice infection, Cefazolin (200 mg/Kg) was dissolved in the animals’ water (25). All procedures were approved by the

Research Ethics Committee of Semnan University of Medical Sciences (IR.SEMUMS.REC.1396.18), which was following the National Institutes of Health (NIH) guidelines for the care and use of laboratory animals (NIH Publications No. 8023, revised Edition 1978).

### 3.3. Ultrasound/Laser Radiation

For ultrasound/laser radiation, the mice were anesthetized, using intraperitoneal ketamine and xylazine. Anesthetized mice with grafted tumors were placed moveless by a specific holder in the near field of ultrasonic waves (30 cm) in a cubic Plexiglas water tank ( $25 \times 25 \times 35 \text{ cm}^3$ ). Two ultrasonic probes (5 cm diameter) were fixed in a  $90^\circ$  position and the central beam of each ultrasound wave was at right angles to the axis of the other. The first source was a 1 MHz (1, 2  $\text{W/cm}^2$ ) and the other source was a 3 MHz (1, 2  $\text{W/cm}^2$ ) ultrasonic treatment system (210P and 215A, Novin Medical Engineering, Isfahan, Iran). The animals were exposed to 150 mW of 650 nm laser light simultaneously with ultrasound, and the time of the ultrasound/laser process was 60 seconds.

### 3.4. Treatment Groups and Tumor Evaluation

The treatment method started when the average diameter of tumors reached 7 mm to 10 mm. To assess the effect of dual-frequency SPDT with injection of sensitizer on breast adenocarcinoma, 132 tumor-bearing female mice were separated randomly into 22 groups ( $n = 6$ ): sham (solvent injection), laser, 4 groups of dual-frequency ultrasound and laser radiation: 1, 3 MHz (1 and 2  $\text{W/cm}^2$ ) + laser, 8 groups of HP-mediated SPDT: 1, 3 MHz (1 and 2  $\text{W/cm}^2$ ) + HP (2.5 and 5 mg/kg) + laser, and 8 groups of HP-MSNs-mediated SPDT: 1, 3 MHz (1 and 2  $\text{W/cm}^2$ ) + HP-MSNs (2.5 and 5 mg/kg) + laser. Due to the weight of experimental mice ( $20 \pm 2 \text{ g}$ ), a dose of 10 mg/kg (0.2 mL) HP, or HP-MSNs were injected intra-peritoneal 24 h before ultrasound (26).

After SPDT performance, to evaluate the tumor volume, the length (a), width (b), and depth (c) of each tumor was measured with a digital caliper every 3 days and mass volume was estimated from the volume formula:  $V = 0.5 \times a \times b \times c$ . The calculated volumes (V) were used to evaluate tumor growth parameters: Relative volume (Relative volume =  $[(V - V_0)/V_0] \times 100$ ), tumor growth inhibition ratio (TGI% =  $[1 - (V_{\text{xday}}/V_{\text{controlday}})] \times 100$ ), and the times needed for each tumor to reach 2 (T2) and 5 times (T5) to the primary mass volume (26). Histopathological images of mass sections were obtained 30 days after the treatment. Tumor sections were stained with hematoxylin/eosin to assess tumor grading and malignancy based on Bloom-Richardson (BR) classification (tumor tubule formation, the number of mitosis/10 high power fields, and nuclear grade). The degree

of tumor grading was low grade (well-differentiated), intermediated grade (moderately-differentiated), and high grade (poorly-differentiated) (27). The histopathological analysis was performed blindly.

### 3.5. Analysis

Statistical analysis was performed, using SPSS 24.0 (SPSS/PC Inc., Chicago, IL, USA). Summary statistics for all normally distributed variables are presented as the mean  $\pm$  standard deviation for each group. One-way analysis of variance (ANOVA) was used for comparison of the mean of independent groups. For multiple comparisons, after one-way ANOVA, we used the Tukey test. Survival analysis was carried out with the Kaplan-Meier and log-rank test for investigating survival times.

## 4. Results

The results obtained from the relative tumor volume after treatment with dual-frequency ultrasound and laser radiation have been plotted in Figure 1. These results indicate that ultrasound and laser radiation have delayed effective tumor growth in comparison with the control and sham groups at 18 days after the treatment. Analysis of data showed non-significant differences between groups before 18 days ( $P > 0.05$ ). Comparison of data showed non-significant differences between groups to reach 2 times and 5 times primary volume in the presence of irradiation ( $P > 0.05$ ). The required time of T2 to the initial volume in groups of dual-frequency ultrasound with 3 MHz (2  $\text{W/cm}^2$ ) radiation was greater than other groups (8 and 6 days, respectively). Analysis of T5 data showed non-significant differences between groups ( $P > 0.05$ ). The inhibition of tumor growth (TGI%) over the experimental period was shown in Figure 2. TGI in the groups that behaved with dual-frequency ultrasound and laser radiation was higher than that of the sham group. The maximum TGI ratio was shown at 18 days after the treatment. The result of the experiment demonstrates that this increase was transient and declined over 30 days of treatment.

To validate our findings, we estimated the anti-tumor effects of HP-mediated SPDT. Figure 3 demonstrates the post-treatment relative tumor volume. Significant differences were detected between experimental groups and sham in tumor volume 15 days after the treatment ( $P < 0.05$ ). Comparison of data showed a non-significant difference between HP-mediated SPDT groups ( $P > 0.05$ ). Investigation of T2 data showed a non-significant difference between HP-mediated SPDT groups ( $P > 0.05$ ). The required time of T5 to the initial volume in groups of 5 mg/kg HP injected was higher than the sham and HP 2.5 mg/kg groups

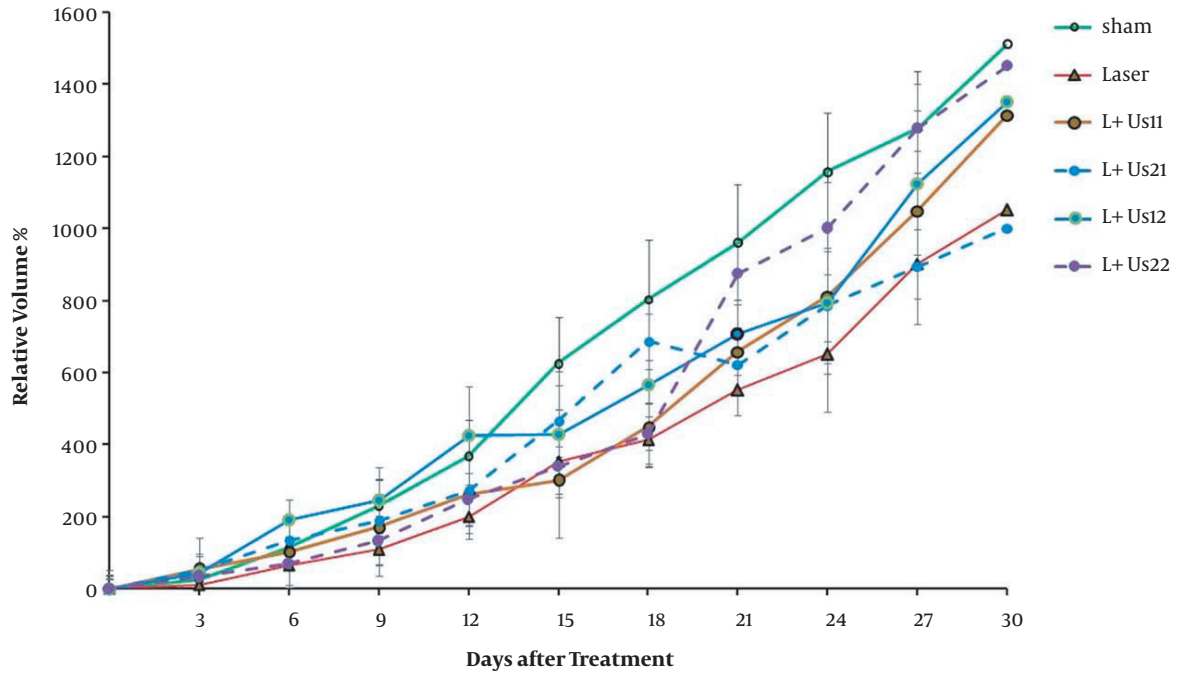


Figure 1. The relative tumor volume of mice adenocarcinoma (mean  $\pm$  SD) for control, sham, laser, and dual-frequency ultrasound (1 and 3 MHz) with laser radiation groups

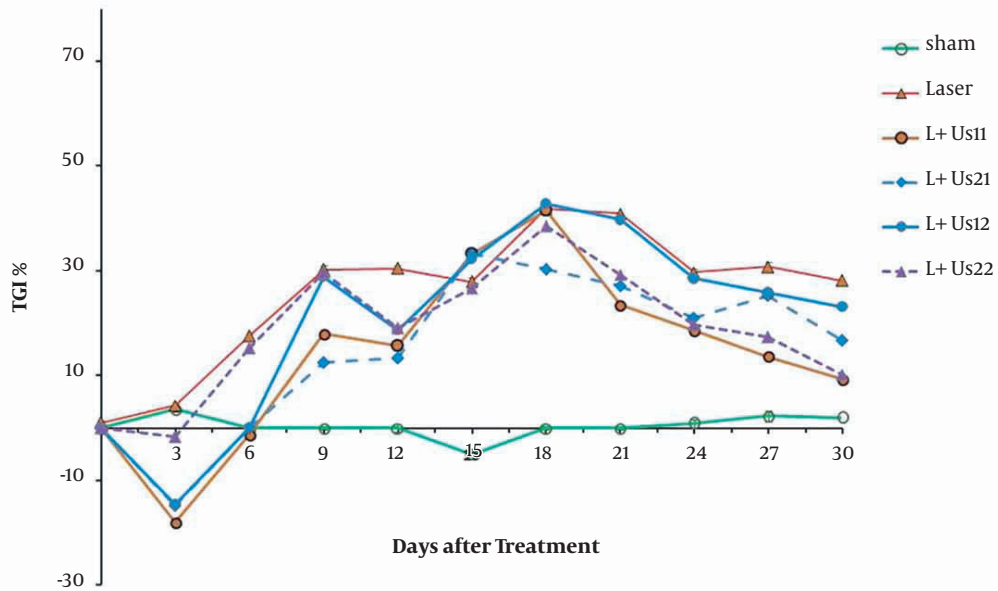


Figure 2. The tumor growth inhibition percent (TGI%) in the experimental groups: Sham, laser, and dual-frequency ultrasound (1 and 3MHz) with laser radiation groups

(18, 14, and 15 days, respectively). As presented in Figure 4, the percent of TGI in the groups of HP-mediated SPDT was greater than that of the sham group. The maximum TGI ratio was shown at 12 days after the treatment. The experiment demonstrates that this increase was not temporary and persisted over 30 days of treatment.

Figure 5 demonstrates tumor growth curves over 30 days after the treatment. These results indicate that HP-MSNs-mediated SPDT is effective in delaying tumor growth when compared with the sham group ( $P < 0.05$ ). Overall comparison of data showed a non-significant difference between SPDT with HP-MSN (2.5 and 5 mg/kg) groups ( $P > 0.05$ ). The time of T2 in the case of HP-MSNs-mediated SPDT groups increased in comparison with sham and that of HP-mediated SPDT groups (13, 6, and 9 days, respectively). In addition, the required time of T5 to the initial volume in all HP-MSNs-mediated SPDT groups was higher than that in the sham and HP-mediated SPDT groups ( $P < 0.05$ ). Furthermore, the T5 time in the trial of dual-frequency SPDT (3 MHz, 2 W/cm<sup>2</sup>) with HP-MSN (5 mg/kg) group rose to 27 days. Figure 6 represents mice breast adenocarcinoma TGI% over 30 days of treatment. TGI in the groups of HP-MSNs-mediated SPDT was higher than that of the sham group ( $P < 0.05$ ). In the groups treated with dual-frequency ultrasound and laser radiation, the maximum TGI ratio was 47.5%, while the maximum TGI ratio in the SPDT groups was 61.6%. The TGI ratio increased in all groups at 12 days after the treatment. Analysis of experimental data demonstrates that this increase was not declined and persisted over 30 days of treatment. The results indicated that HP-mediated and HP-MSNs-mediated SPDT are effective in relative tumor volume when compared with the sham group ( $447.7 \pm 119$ ,  $339.1 \pm 161$ , and  $1510.8 \pm 160$ , respectively).

Kaplan-Meier analysis of experimental data revealed that the 72 days survival (cumulative survival fraction) was 95% for the 5 mg/kg HP-MSNs-mediated SPDT group. The survival meantime (with 95% confidence interval) for the sham, laser, dual-frequency ultrasound, HP-mediated SPDT (5 mg/kg) groups was 32, 34, 35, and 51 days, respectively; the overall comparison test of survival equality for the different levels of groups demonstrated a significant difference between experimental groups: Log Rank (Mantel-Cox),  $P = 0.014$ .

Microscopically assessment of tumor sections revealed multiple nuclear mitosis and polymorphism in all investigational groups (Figure 7). The results of the histopathological study to determine the grading of the tumor were shown in Table 1. The sham and laser groups had grade III malignancy (poorly differentiated), while HP-MSNs-mediated SPDT groups had grade II malignancy (well-differentiated) in the histological study of mice breast adeno-

nocarcinoma.

## 5. Discussion

The results of the above-mentioned experiments show that the combined dual-frequency ultrasound (1 + 3 MHz) and/or laser (650 nm) radiation caused a transient inhibition effect on mice breast adenocarcinoma tumor growth. Also, HP-mediated SPDT (2.5 and 5 mg/kg) caused anti-tumor effect. Moreover, HP-MSNs-mediated SPDT (2.5 and 5 mg/kg) had inhibition effect on tumor growth. The TGI ratio increased in all experimental groups at 12 days after the initiation of radiation and persisted over 30 days of treatment. These findings are in agreement with Barati et al.'s findings that dual ultrasound (1 MHz + 150 kHz) for 30 min decreased mice breast adenocarcinoma tumor growth (28). In addition, Guan and Xu showed that high-intensity focused ultrasound (1.6 MHz) could destroy proliferating tumor cells in human breast cancer (29). In agreement with our results, the findings of Banerjee et al. confirm a potential role for PDT with verteporfin and laser (690 nm) in the management of early breast cancer in 12 female patients (1). Miyoshi et al. suggested that combination therapy of SDT (titanium oxide)/PDT (aminolevulinic acid) can help to get a reasonable anti-tumor effect on mice squamous cell carcinoma because the ultrasound (1 MHz) deeper penetration into the cancer tissue was compared with the laser light (635 nm) (5). Moreover, the findings demonstrated that chlorin e6-mediated SPDT enhanced the antitumor efficacy on 4T1 mammary cancer cells compared with SDT (1 MHz) and PDT (laser 650 nm) alone (30). The combination of PDT (665 nm) and SDT (3.3 MHz) have shown an improved glioblastoma cell in vitro and in vivo, which could be referred to as a synergetic effect. Exposing the nano-formulation HPPH with ultrasound also triggered the release of PS (31). In An et al.'s study, a 630 nm semiconductor laser and 1 MHz ultrasound were used to perform SPDT. In An et al.'s study, SPDT with 630 nm laser and 1 MHz ultrasound + sinoporphyrin sodium inhibited glioma cell proliferation and induced cell apoptosis due to the generation of ROS and affecting protein expression (32). Moreover, Hong et al. proposed SPDT with a nanoformulation Ce6-P/WNE in the treatment of prostate cancer cells. The results concluded that activated Ce6-P/WNEs in tumor cells by light (633 nm) and/or ultrasound (2.1 MHz) produced ROS even in a hypoxic environment (19).

The structure of mesoporous channels would allow controllable drug release by mechanical and cavitation effects of ultrasound (33). The collapse of cavitating bubbles can cause sonomechanical and sonochemical cytotoxic effects and the formation of cytotoxic reactive oxygen

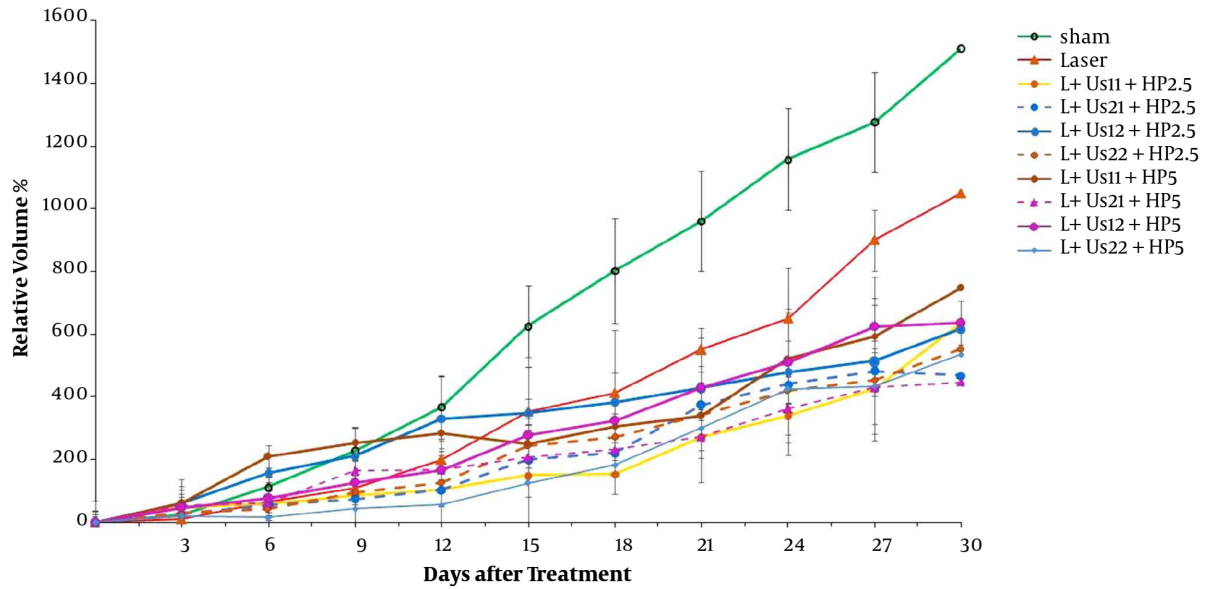


**Figure 3.** The relative tumor volume percent of mice breast adenocarcinoma (mean  $\pm$  SD) for the experimental groups: Sham, laser, and HP-mediated SPDT (2.5 and 5 mg/kg) groups

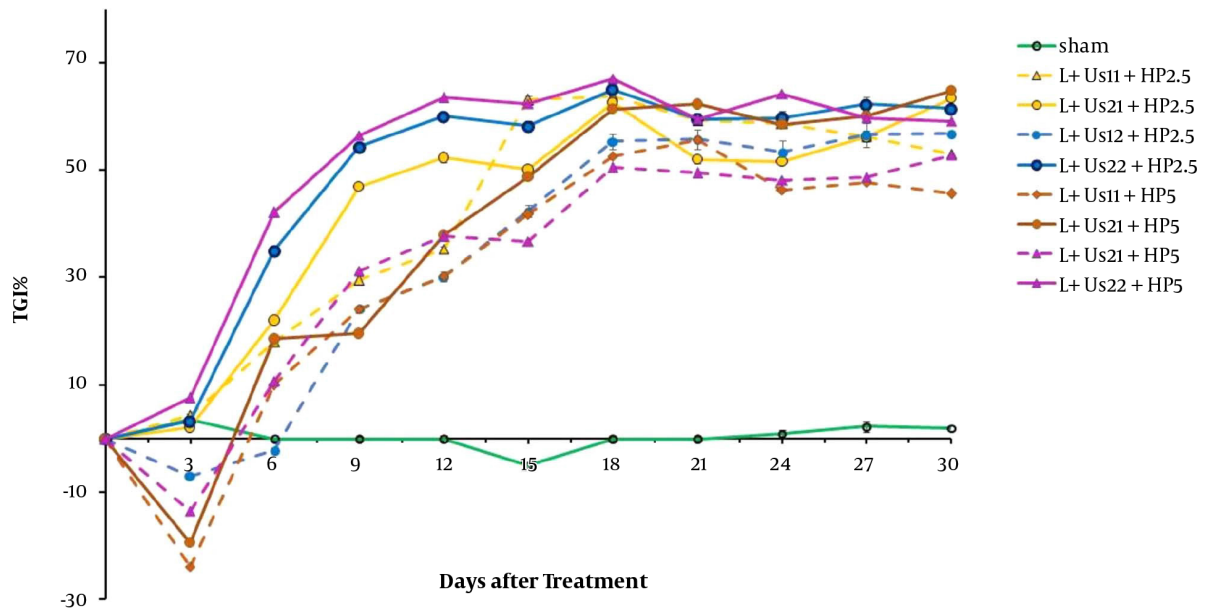


**Figure 4.** The tumor growth inhibition percent (TGI%) in the following treatment groups: Sham, laser, and HP-mediated SPDT (2.5 and 5 mg/kg) groups

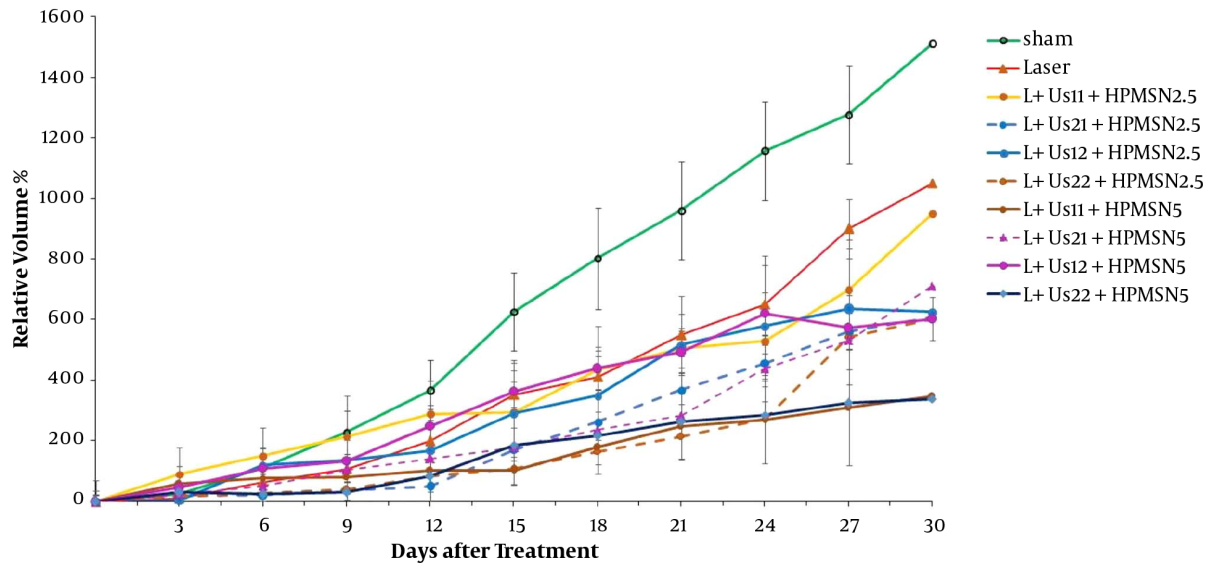


**Figure 5.** The relative tumor volume percent of mice breast adenocarcinoma (mean  $\pm$  SD) for the experimental groups: Sham, laser, and HP-MSNs-mediated SPDT (2.5 and 5 mg/kg) groups

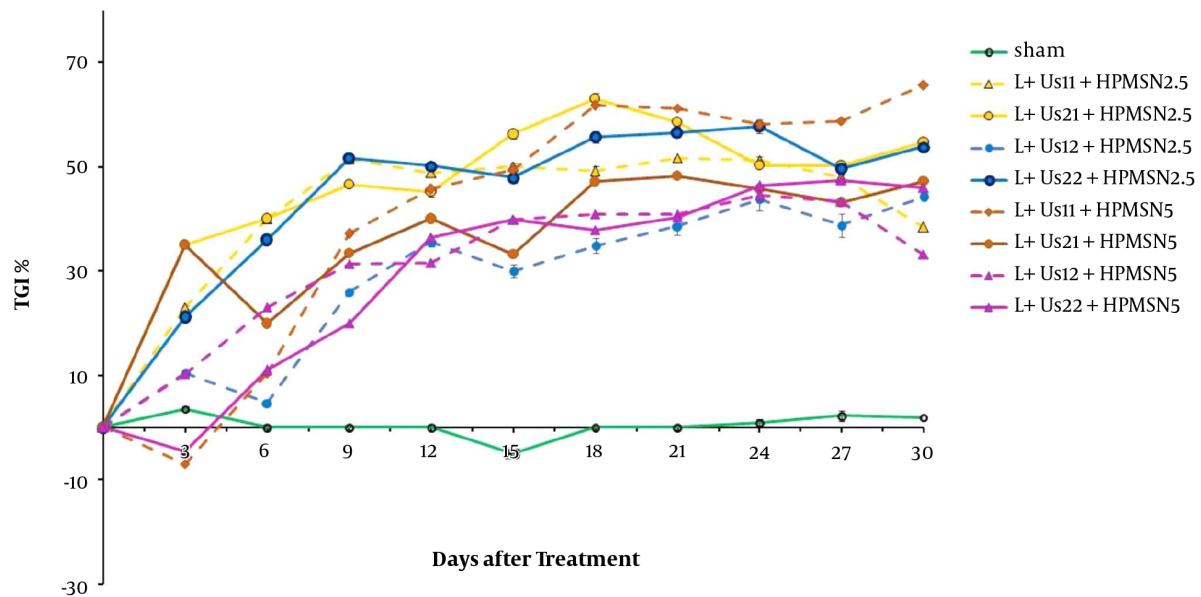


**Figure 6.** The tumor growth inhibition percent (TGI%) in the following treatment groups: Sham, laser, and HP-MSNs-mediated SPDT (2.5 and 5 mg/kg) groups

species (34). Hence, this means that a combination of ultrasound and HP-MSNs could have a better treatment effect on mice breast adenocarcinoma. In agreement with our findings, Zhang et al. investigated that the therapeutic effect of encapsulated HP-SDT was better than HP or ultrasound alone (35). In addition, during a study by Hasanzadeh et

al. to review the effect of dual-frequency ultrasound radiation on nanomicellar containing doxorubicin, the SDT increased the ultrasound cavitations' efficiency (13).

Cellular antioxidant capacity reduction may cause by oxidative stress. Free radical formation impairs the cell membrane fatty acids and proteins' function. As well, free

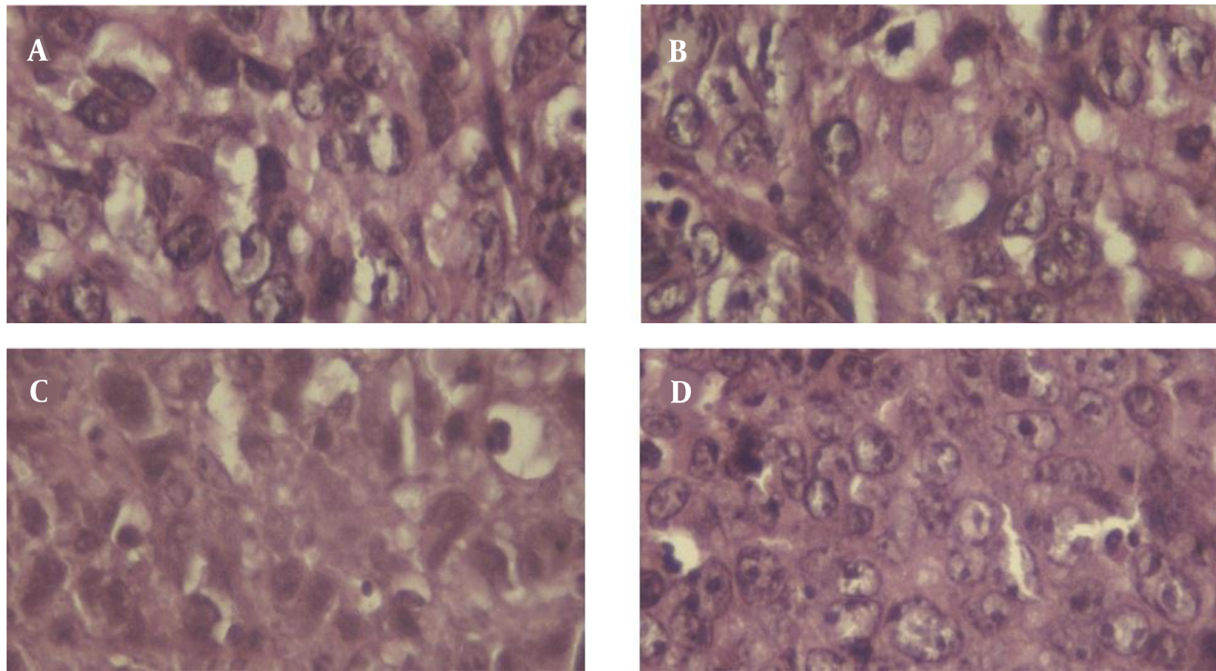


**Figure 7.** Histopathological images of tumor tissue sections; A, sham; B, laser; C, HP-mediated SPDT (5 mg/kg); and D, HP-MSNs-mediated SPDT (5 mg/kg) groups

**Table 1.** The Properties of Mice Breast Adenocarcinoma Based on Bloom-Richardson (BR) Classification in the Sham, Laser, Dual-Frequency Ultrasound and Laser Radiation, HP-mediated SPDT (5 mg/kg), and HP-MSNs-mediated SPDT (5 mg/kg) Experimental Groups

Group	Tumor Tubule Formation	Number of Mitosis	Total Score	BR Grade	BR Grade	Grade
Sham	3	3	3	9	Poorly differentiated	3
Laser	3	3	3	9	Poorly differentiated	3
Laser + US22	1	3	3	7	Moderately differentiated	1
Laser + US22 + HP5	2	2	2	5	Well differentiated	1
Laser + US22 + HPMSN5	1	2	1	4	Well differentiated	1

radical production reacts with gene mutation and DNA damage, which provokes cancer development (36). PDT applies its effects when the light is used to activate a photochemical reaction of a non-toxic PS, which generates reactive oxygen species (ROS). These ROS cause oxidative damage to lipids, proteins, and nucleic acids, which lead to the destruction of cancer cells through apoptosis or necrosis. The mentioned constructions have strong light absorption at wavelengths > 650 nm and are essential for good tissue penetration of light (37). The destruction effect of PDT not only depends on the type of PS, but also is related to light exposure and fluency, oxygen level, localization of sensitizer, drug administration time, and other parameters (38). Despite the satisfactory advantages of PDT, the clinical application of this approach has been limited. Several reasons can be explained such as the poor penetration of light

and its dependence on the tumor tissue oxygen presence (39).

Ultrasound good tissue penetration and wave energy focusing on the depth of tumor tissue can produce bio-effects (11). It mentioned that acoustic cavitation is the main cause of destructive chemical reactions and the free radical production since ultrasound irradiation. During a study by Feng et al., the effect of mixing two-frequency and three-frequency ultrasonic waves on cavitations' efficiency was investigated. The results showed that irradiation of two or more ultrasound waves significantly increases the cavitations' efficiency compared to single-frequency irradiation (40). The simultaneous effects of sensitizer and ultrasound comprise mechanical, chemical, and cavitation mechanisms (28). Protoporphyrin that is used in PDT can generate active oxygen species after activation by visible



light (41). SDT followed by PDT can help to get a realistic anti-tumor effect because ultrasound has deeper penetration into the tumor tissue compared to laser light. Besides the singlet oxygen mechanism in PDT, mechanical stress, cavitation effects, and reactive oxygen species comprise SDT (4).

The histopathological results (Bloom-Richardson classification basis) showed that the sham and laser groups had grade III malignancy (poorly differentiated), while HP-mediated SPDT and HP-MSNs-mediated SPDT groups had grade I malignancy (well-differentiated) in the histological study of mice breast adenocarcinoma. Overall comparison test of survival equality for the different levels of groups demonstrated a significant difference between groups: Log rank (Mantel-Cox),  $P = 0.014$ . This may cause simultaneous radiation of dual-frequency ultrasound and laser radiation. On contrary, analysis of the author's previous investigation revealed that injection of HP and HP-MSNs (2.5 mg/kg) did not show any effect on T2 time and tumor relative volume, and the tumors had a poorly differentiated grading. The results of single-frequency SDT were not only determined by ultrasound wave power density, but also were related to HP-MSN injected dose (25). Hong et al.'s study demonstrated that to overcome the limitations of each modality in the hypoxia environment, the strengths of PDT and SDT could be combined. The ultrasound deep tissue penetration combined with sensitizer activation by light will significantly enhance the therapeutic applications for prostate cancer cells (19). In theory, the tumor cell toxicity effects of SDT and PDT are facilitated by cytotoxic drugs that are produced by sonochemical or photochemical reactions (42).

The opinion of SPDT is based on the special buildup of sensitizer in tumors, and the improved cytotoxicity after activation by ultrasound or light. The imaginable tumor uptake could be explained as (1) selective buildup related to the tumor surrounding microenvironment, (2) lipoprotein receptors in some of the tumor cells, and (3) endocytosis mechanism to the entrance of sensitizer and low-density protein binding. In addition, because of the lower pH value in tumors, tumor-associated macrophages receive large amounts of porphyrin derivatives (4). SPDT has been used in the treatment of many cancers with variable success, but the efficacy of breast adenocarcinoma damage induced by dual-frequency SPDT with HP-MSNs has rarely been reported. The novelty of the present SPDT study was activation of HP and HP-MSNs (2.5 and 5 mg/kg) in the presence of two intensities (1 and 2 W/cm<sup>2</sup>) of 1 and 3 MHz ultrasound and laser radiation (650 nm) in the management of Inbred Balb/C mice grafted breast adenocarcinoma. Aside from only one laser light radiation (650 nm), another limitation of this research was once sensitizer injection with

a temporary treatment effect. The fractional injection of sensitizer should be done in our future study.

### 5.1. Conclusions

The results of this study demonstrated that HP and HP-MSNs-mediated SPDT have an anti-tumor effect in mice breast adenocarcinoma. It can be appreciated that careful selection of the sensitizer with SPDT will play an eminent role in the success of cancer therapies. Improvement sensitizer agents used in PDT and SDT are useful drugs for SPDT and can expand cancer treatment management. However, further studies are required to optimize the sensitizer, light/laser, and ultrasound parameters to find better tumor treatment methods and explain the mechanism of SPDT.

### Acknowledgments

We would like to thank the Semnan University of Medical Sciences and the Medical Physics Department for their cooperation to make available facilities for this work.

### Footnotes

**Authors' Contribution:** Study concept and design: H. H.; acquisition of data: T. Kh., Sh. M., Sh. S., and Sh. Sh.; analysis and interpretation of data: H. H., and M. J.; drafting of the manuscript: M. J.; critical revision of the manuscript for important intellectual content: M. J.; statistical analysis: R. Gh.

**Conflict of Interests:** The authors certify that they have no affiliations with or involvement in any organization or entity with any financial interest in the subject matter or materials discussed in this manuscript. All the authors declare that they have no conflict of interest.

**Data Reproducibility:** The data presented in this study are openly available in one of the repositories or will be available on request from the corresponding author by this journal representative at any time during submission or after publication. Otherwise, all consequences of possible withdrawal or future retraction will be with the corresponding author.

**Ethical Approval:** All procedures were approved by the Research Ethics Committee of Semnan University of Medical Sciences (IR.SEMUMS.REC.1396.18), which was following the National Institutes of Health (NIH) guidelines for the care and use of laboratory animals (NIH Publications No. 8023, revised Edition 1978).

**Funding/Support:** This work was supported by Semnan University of Medical Sciences (1217).

## References

- Banerjee SM, El-Sheikh S, Malhotra A, Mosse CA, Parker S, Williams NR, et al. Photodynamic Therapy in Primary Breast Cancer. *J Clin Med*. 2020;**9**(2). doi: [10.3390/jcm9020483](https://doi.org/10.3390/jcm9020483). [PubMed: [32050675](https://pubmed.ncbi.nlm.nih.gov/32050675/)]. [PubMed Central: [PMC7074474](https://pubmed.ncbi.nlm.nih.gov/PMC7074474/)].
- Dos Santos AF, De Almeida DRQ, Terra LF, Baptista MS, Labriola L. Photodynamic therapy in cancer treatment - an update review. *J. cancer metastasis treat*. 2019;**2019**. doi: [10.20517/2394-4722.2018.83](https://doi.org/10.20517/2394-4722.2018.83).
- Allison RR, Moghissi K. Photodynamic Therapy (PDT): PDT Mechanisms. *Clin Endosc*. 2013;**46**(1):24-9. doi: [10.5946/ce.2013.46.1.24](https://doi.org/10.5946/ce.2013.46.1.24). [PubMed: [23422955](https://pubmed.ncbi.nlm.nih.gov/23422955/)]. [PubMed Central: [PMC3572346](https://pubmed.ncbi.nlm.nih.gov/PMC3572346/)].
- Mai B, Wang X, Liu Q, Zhang K, Wang P. The Application of DVDMS as a Sensitizing Agent for Sono-/Photo-Therapy. *Front Pharmacol*. 2020;**11**:19. doi: [10.3389/fphar.2020.00019](https://doi.org/10.3389/fphar.2020.00019). [PubMed: [32116698](https://pubmed.ncbi.nlm.nih.gov/32116698/)]. [PubMed Central: [PMC7020569](https://pubmed.ncbi.nlm.nih.gov/PMC7020569/)].
- Miyoshi N, Kundu SK, Tuziuti T, Yasui K, Shimada I, Ito Y. Combination of Sonodynamic and Photodynamic Therapy against Cancer Would Be Effective through Using a Regulated Size of Nanoparticles. *Nanosci Nanoeng*. 2016;**4**(1):1-11. doi: [10.13189/nn.2016.040101](https://doi.org/10.13189/nn.2016.040101). [PubMed: [27088115](https://pubmed.ncbi.nlm.nih.gov/27088115/)]. [PubMed Central: [PMC4827930](https://pubmed.ncbi.nlm.nih.gov/PMC4827930/)].
- Sibata CH, Colussi VC, Oleinick NL, Kinsella TJ. Photodynamic therapy: a new concept in medical treatment. *Braz J Med Biol Res*. 2000;**33**(8):869-80. doi: [10.1590/s0100-879x2000008000002](https://doi.org/10.1590/s0100-879x2000008000002). [PubMed: [11023333](https://pubmed.ncbi.nlm.nih.gov/11023333/)].
- Secret E, Maynadier M, Gallud A, Gary-Bobo M, Chaix A, Belamie E, et al. Anionic porphyrin-grafted porous silicon nanoparticles for photodynamic therapy. *Chem Commun (Camb)*. 2013;**49**(39):4202-4. doi: [10.1039/c3cc38837a](https://doi.org/10.1039/c3cc38837a). [PubMed: [23558261](https://pubmed.ncbi.nlm.nih.gov/23558261/)].
- Banerjee SM, MacRobert AJ, Mosse CA, Periera B, Bown SG, Keshtgar MRS. Photodynamic therapy: Inception to application in breast cancer. *Breast*. 2017;**31**:105-13. doi: [10.1016/j.breast.2016.09.016](https://doi.org/10.1016/j.breast.2016.09.016). [PubMed: [27833041](https://pubmed.ncbi.nlm.nih.gov/27833041/)].
- Chen H, Zhou X, Gao Y, Zheng B, Tang F, Huang J. Recent progress in development of new sonosensitizers for sonodynamic cancer therapy. *Drug Discov Today*. 2014;**19**(4):502-9. doi: [10.1016/j.drudis.2014.01.010](https://doi.org/10.1016/j.drudis.2014.01.010). [PubMed: [24486324](https://pubmed.ncbi.nlm.nih.gov/24486324/)].
- McHale AP, Callan JF, Nomikou N, Fowley C, Callan B. Sonodynamic Therapy: Concept, Mechanism and Application to Cancer Treatment. *Adv Exp Med Biol*. 2016;**880**:429-50. doi: [10.1007/978-3-319-22536-4\\_22](https://doi.org/10.1007/978-3-319-22536-4_22). [PubMed: [26486350](https://pubmed.ncbi.nlm.nih.gov/26486350/)].
- Rosenthal I, Sostarik JZ, Riesz P. Sonodynamic therapy—a review of the synergistic effects of drugs and ultrasound. *Ultrason Sonochem*. 2004;**11**(6):349-63. doi: [10.1016/j.ultsonch.2004.03.004](https://doi.org/10.1016/j.ultsonch.2004.03.004). [PubMed: [15302020](https://pubmed.ncbi.nlm.nih.gov/15302020/)].
- Shibaguchi H, Tsuru H, Kuroki M, Kuroki M. Sonodynamic cancer therapy: a non-invasive and repeatable approach using low-intensity ultrasound with a sonosensitizer. *Anticancer Res*. 2011;**31**(7):2425-9. [PubMed: [21873154](https://pubmed.ncbi.nlm.nih.gov/21873154/)].
- Hasanzadeh H, Mokhtari-Dizaji M, Zahra Bathaie S, Hassan ZM, Shahbazfar AA. Dual-frequency ultrasound activation of nanomicellar doxorubicin in targeted tumor chemotherapy. *J Med Ultrason (2001)*. 2014;**41**(2):139-50. doi: [10.1007/s10396-013-0484-x](https://doi.org/10.1007/s10396-013-0484-x). [PubMed: [2727765](https://pubmed.ncbi.nlm.nih.gov/2727765/)].
- Wan GY, Liu Y, Chen BW, Liu YY, Wang YS, Zhang N. Recent advances of sonodynamic therapy in cancer treatment. *Cancer Biol Med*. 2016;**13**(3):325-38. doi: [10.20892/j.issn.2095-3941.2016.0068](https://doi.org/10.20892/j.issn.2095-3941.2016.0068). [PubMed: [27807500](https://pubmed.ncbi.nlm.nih.gov/27807500/)]. [PubMed Central: [PMC5069838](https://pubmed.ncbi.nlm.nih.gov/PMC5069838/)].
- Wang T, Zhang L, Su Z, Wang C, Liao Y, Fu Q. Multifunctional hollow mesoporous silica nanocages for cancer cell detection and the combined chemotherapy and photodynamic therapy. *ACS Appl Mater Interfaces*. 2011;**3**(7):2479-86. doi: [10.1021/am200364e](https://doi.org/10.1021/am200364e). [PubMed: [21604817](https://pubmed.ncbi.nlm.nih.gov/21604817/)].
- Zheng Y, Zhang Y, Ao M, Zhang P, Zhang H, Li P, et al. Hematoporphyrin encapsulated PLGA microbubble for contrast enhanced ultrasound imaging and sonodynamic therapy. *J Microencapsul*. 2012;**29**(5):437-44. doi: [10.3109/02652048.2012.655333](https://doi.org/10.3109/02652048.2012.655333). [PubMed: [22299595](https://pubmed.ncbi.nlm.nih.gov/22299595/)].
- Yang KN, Zhang CQ, Wang W, Wang PC, Zhou JP, Liang XJ. pH-responsive mesoporous silica nanoparticles employed in controlled drug delivery systems for cancer treatment. *Cancer Biol Med*. 2014;**11**(1):34-43. doi: [10.7497/j.issn.2095-3941.2014.01.003](https://doi.org/10.7497/j.issn.2095-3941.2014.01.003). [PubMed: [24738037](https://pubmed.ncbi.nlm.nih.gov/24738037/)]. [PubMed Central: [PMC3969802](https://pubmed.ncbi.nlm.nih.gov/PMC3969802/)].
- Xu Z, Liu S, Kang Y, Wang M. Glutathione- and pH-responsive non-porous silica prodrug nanoparticles for controlled release and cancer therapy. *Nanoscale*. 2015;**7**(13):5859-68. doi: [10.1039/c5nr00297d](https://doi.org/10.1039/c5nr00297d). [PubMed: [25757484](https://pubmed.ncbi.nlm.nih.gov/25757484/)].
- Hong L, Pliss AM, Zhan Y, Zheng W, Xia J, Liu L, et al. Perfluoropolyether Nanoemulsion Encapsulating Chlorin e6 for Sonodynamic and Photodynamic Therapy of Hypoxic Tumor. *Nanomaterials (Basel)*. 2020;**10**(10). doi: [10.3390/nano10102058](https://doi.org/10.3390/nano10102058). [PubMed: [33086490](https://pubmed.ncbi.nlm.nih.gov/33086490/)]. [PubMed Central: [PMC7603101](https://pubmed.ncbi.nlm.nih.gov/PMC7603101/)].
- Alamolhoda M, Mokhtari-Dizaji M, Barati AH, Hasanzadeh H. Erratum to: Comparing the in vivo sonodynamic effects of dual- and single-frequency ultrasound in breast adenocarcinoma. *J Med Ultrason (2001)*. 2012;**39**(4):291. doi: [10.1007/s10396-012-0391-6](https://doi.org/10.1007/s10396-012-0391-6). [PubMed: [27279121](https://pubmed.ncbi.nlm.nih.gov/27279121/)].
- Kanthale PM, Brotchie A, Ashokkumar M, Grieser F. Experimental and theoretical investigations on sonoluminescence under dual frequency conditions. *Ultrason Sonochem*. 2008;**15**(4):629-35. doi: [10.1016/j.ultsonch.2007.08.006](https://doi.org/10.1016/j.ultsonch.2007.08.006). [PubMed: [17931950](https://pubmed.ncbi.nlm.nih.gov/17931950/)].
- Hasanzadeh H, Mokhtari-Dizaji M, Bathaie SZ, Hassan ZM. Effect of local dual frequency sonication on drug distribution from polymeric nanomicelles. *Ultrason Sonochem*. 2011;**18**(5):1165-71. doi: [10.1016/j.ultsonch.2011.03.018](https://doi.org/10.1016/j.ultsonch.2011.03.018). [PubMed: [21489850](https://pubmed.ncbi.nlm.nih.gov/21489850/)].
- Yu X, Trase I, Ren M, Duval K, Guo X, Chen Z. Design of Nanoparticle-Based Carriers for Targeted Drug Delivery. *J Nanomater*. 2016;**2016**. doi: [10.1155/2016/1087250](https://doi.org/10.1155/2016/1087250). [PubMed: [27398083](https://pubmed.ncbi.nlm.nih.gov/27398083/)]. [PubMed Central: [PMC4936496](https://pubmed.ncbi.nlm.nih.gov/PMC4936496/)].
- Vazquez NI, Gonzalez Z, Ferrari B, Castro Y. Synthesis of mesoporous silica nanoparticles by sol-gel as nanocontainer for future drug delivery applications. *Bol. Soc. Esp. Ceram. Vidr*. 2017;**56**(3):139-45. doi: [10.1016/j.bsecv.2017.03.002](https://doi.org/10.1016/j.bsecv.2017.03.002).
- Jafari S, Jadidi M, Hasanzadeh H, Khani T, Nasr R, Semnani V. Sonodynamic Therapy of Mice Breast Adenocarcinoma with HP-MSN. *Iran J Sci Technol Trans A Sci*. 2020;**44**(3):651-60. doi: [10.1007/s40995-020-00893-5](https://doi.org/10.1007/s40995-020-00893-5).
- Alamolhoda M, Mokhtari-Dizaji M. Evaluation of fractionated and repeated sonodynamic therapy by using dual frequency for murine model of breast adenocarcinoma. *J Ther Ultrasound*. 2015;**3**:10. doi: [10.1186/s40349-015-0031-x](https://doi.org/10.1186/s40349-015-0031-x). [PubMed: [26124951](https://pubmed.ncbi.nlm.nih.gov/26124951/)]. [PubMed Central: [PMC4484850](https://pubmed.ncbi.nlm.nih.gov/PMC4484850/)].
- Bloom HJ, Richardson WW. Histological grading and prognosis in breast cancer; a study of 1409 cases of which 359 have been followed for 15 years. *Br J Cancer*. 1957;**11**(3):359-77. doi: [10.1038/bjc.1957.43](https://doi.org/10.1038/bjc.1957.43). [PubMed: [13499785](https://pubmed.ncbi.nlm.nih.gov/13499785/)]. [PubMed Central: [PMC2073885](https://pubmed.ncbi.nlm.nih.gov/PMC2073885/)].
- Barati AH, Mokhtari-Dizaji M, Mozdarani H, Bathaie Z, Hassan ZM. Effect of exposure parameters on cavitation induced by low-level dual-frequency ultrasound. *Ultrason Sonochem*. 2007;**14**(6):783-9. doi: [10.1016/j.ultsonch.2006.12.016](https://doi.org/10.1016/j.ultsonch.2006.12.016). [PubMed: [17347019](https://pubmed.ncbi.nlm.nih.gov/17347019/)].
- Guan L, Xu G. Damage effect of high-intensity focused ultrasound on breast cancer tissues and their vascularities. *World J Surg Oncol*. 2016;**14**(1):153. doi: [10.1186/s12957-016-0908-3](https://doi.org/10.1186/s12957-016-0908-3). [PubMed: [27230124](https://pubmed.ncbi.nlm.nih.gov/27230124/)]. [PubMed Central: [PMC4882851](https://pubmed.ncbi.nlm.nih.gov/PMC4882851/)].
- Li Q, Wang X, Wang P, Zhang K, Wang H, Feng X, et al. Efficacy of chlorin e6-mediated sono-photodynamic therapy on 4T1 cells. *Cancer Biother Radiopharm*. 2014;**29**(1):42-52. doi: [10.1089/cbr.2013.1526](https://doi.org/10.1089/cbr.2013.1526). [PubMed: [24206161](https://pubmed.ncbi.nlm.nih.gov/24206161/)]. [PubMed Central: [PMC3869416](https://pubmed.ncbi.nlm.nih.gov/PMC3869416/)].
- Borah BM, Cacaccio J, Durrani FA, Bshara W, Turowski SG, Sperryak JA, et al. Sonodynamic therapy in combination with photodynamic therapy shows enhanced long-term cure of brain tumor. *Sci Rep*.

- 2020;**10**(1):21791. doi: [10.1038/s41598-020-78153-0](https://doi.org/10.1038/s41598-020-78153-0). [PubMed: [33311561](https://pubmed.ncbi.nlm.nih.gov/33311561/)]. [PubMed Central: [PMC7732989](https://pubmed.ncbi.nlm.nih.gov/PMC7732989/)].
32. An YW, Liu HQ, Zhou ZQ, Wang JC, Jiang GY, Li ZW, et al. Sino- porphyrin sodium is a promising sensitizer for photodynamic and sonodynamic therapy in glioma. *Oncol Rep.* 2020;**44**(4):1596–604. doi: [10.3892/or.2020.7695](https://doi.org/10.3892/or.2020.7695). [PubMed: [32945475](https://pubmed.ncbi.nlm.nih.gov/32945475/)]. [PubMed Central: [PMC7448408](https://pubmed.ncbi.nlm.nih.gov/PMC7448408/)].
33. Wang J, Jiao Y, Shao Y. Mesoporous Silica Nanoparticles for Dual-Mode Chemo-Sonodynamic Therapy by Low-Energy Ultrasound. *Materials (Basel).* 2018;**11**(10). doi: [10.3390/ma11102041](https://doi.org/10.3390/ma11102041). [PubMed: [30347751](https://pubmed.ncbi.nlm.nih.gov/30347751/)]. [PubMed Central: [PMC6212853](https://pubmed.ncbi.nlm.nih.gov/PMC6212853/)].
34. Canavese G, Ancona A, Racca L, Canta M, Dumontel B, Barbaresco F, et al. Nanoparticle-assisted ultrasound: A special focus on sonodynamic therapy against cancer. *Chem Eng J.* 2018;**340**:155–72. doi: [10.1016/j.cej.2018.01.060](https://doi.org/10.1016/j.cej.2018.01.060). [PubMed: [30881202](https://pubmed.ncbi.nlm.nih.gov/30881202/)]. [PubMed Central: [PMC6420022](https://pubmed.ncbi.nlm.nih.gov/PMC6420022/)].
35. Zhang Y, Ou Y, Guo J, Huang X. Ultrasound-triggered breast tumor sonodynamic therapy through hematoporphyrin monomethyl ether-loaded liposome. *J Biomed Mater Res B Appl Biomater.* 2020;**108**(3):948–57. doi: [10.1002/jbm.b.34447](https://doi.org/10.1002/jbm.b.34447). [PubMed: [31389180](https://pubmed.ncbi.nlm.nih.gov/31389180/)].
36. Ronco AL, Martínez-López W, Mendoza B, Calderón JM. Epidemiologic Evidence for Association between a High Dietary Acid Load and the Breast Cancer Risk. *SciMed. J.* 2021;**3**(2):166–76. doi: [10.28991/SciMedJ-2021-0302-8](https://doi.org/10.28991/SciMedJ-2021-0302-8).
37. Silva ZS, Bussadori SK, Fernandes KP, Huang YY, Hamblin MR. Animal models for photodynamic therapy (PDT). *Biosci Rep.* 2015;**35**(6). doi: [10.1042/BSR20150188](https://doi.org/10.1042/BSR20150188). [PubMed: [26415497](https://pubmed.ncbi.nlm.nih.gov/26415497/)]. [PubMed Central: [PMC4643327](https://pubmed.ncbi.nlm.nih.gov/PMC4643327/)].
38. Aniogo EC, Plackal Adimuriyil George B, Abrahamse H. The role of photodynamic therapy on multidrug resistant breast cancer. *Cancer Cell Int.* 2019;**19**:91. doi: [10.1186/s12935-019-0815-0](https://doi.org/10.1186/s12935-019-0815-0). [PubMed: [31007609](https://pubmed.ncbi.nlm.nih.gov/31007609/)]. [PubMed Central: [PMC6458738](https://pubmed.ncbi.nlm.nih.gov/PMC6458738/)].
39. Vega DL, Lodge P, Vivero-Escoto JL. Redox-Responsive Porphyrin-Based Polysilsesquioxane Nanoparticles for Photodynamic Therapy of Cancer Cells. *Int J Mol Sci.* 2015;**17**(1). doi: [10.3390/ijms17010056](https://doi.org/10.3390/ijms17010056). [PubMed: [26729110](https://pubmed.ncbi.nlm.nih.gov/26729110/)]. [PubMed Central: [PMC4730301](https://pubmed.ncbi.nlm.nih.gov/PMC4730301/)].
40. Feng R, Zhao Y, Zhu C, Mason TJ. Enhancement of ultrasonic cavitation yield by multi-frequency sonication. *Ultrason Sonochem.* 2002;**9**(5):231–6. doi: [10.1016/s1350-4177\(02\)00083-4](https://doi.org/10.1016/s1350-4177(02)00083-4). [PubMed: [12371198](https://pubmed.ncbi.nlm.nih.gov/12371198/)].
41. Sadanala KC, Chaturvedi PK, Seo YM, Kim JM, Jo YS, Lee YK, et al. Sono- photodynamic combination therapy: a review on sensitizers. *Anti- cancer Res.* 2014;**34**(9):4657–64. [PubMed: [25202041](https://pubmed.ncbi.nlm.nih.gov/25202041/)].
42. Huang Z, Moseley H, Bown S. Rationale of combined PDT and SDT modalities for treating cancer patients in terminal stage: the proper use of photosensitizer. *Integr Cancer Ther.* 2010;**9**(4):317–9. discussion 320-1. doi: [10.1177/1534735410384858](https://doi.org/10.1177/1534735410384858). [PubMed: [21106611](https://pubmed.ncbi.nlm.nih.gov/21106611/)].